# On the Stability of Selected Hydrogen-bonded Semiconductors in Organic Electronics Devices

Mihai Irimia-Vladu*, Yasin Kanbur, Fausta Camaioni, Maria Elisabetta Coppola, Cigdem Yumusak, Cristian Vlad Irimia, Angela Vlad, Alessandra Operamolla, Gianluca M. Farinola, Gian Paolo Suranna, Natalia González-Benitez, María Carmen Molina, Luis Fernando Bautista, Heinz Langhals, Barbara Stadlober, Eric Daniel Głowacki, Niyazi Serdar Sariciftci

CORRESPONDING AUTHOR: Mihai Irimia-Vladu: mihai.irimiavladu@gmail.com

## -Supplementary Information-

When describing dyes and pigments, one necessarily refers to the colour that characterizes these types of compounds. The scientific definition of colour is the visual perception generated by the nervous signals that the photoreceptors on the retina of the eye send to the brain when they absorb electromagnetic radiation of certain wavelengths and intensities.

Both Alizarin and Indigo dyes were extracted from plants, but the dying process was completely different for the two dyestuffs. Alizarin, originating from the roots of the plant dyer's madder (*Rubia tinctorum*) was applied as mordant dye to form complexes with a metal, preferently aluminium, where the latter was linked to the textile fibre to form a rather stable dying.

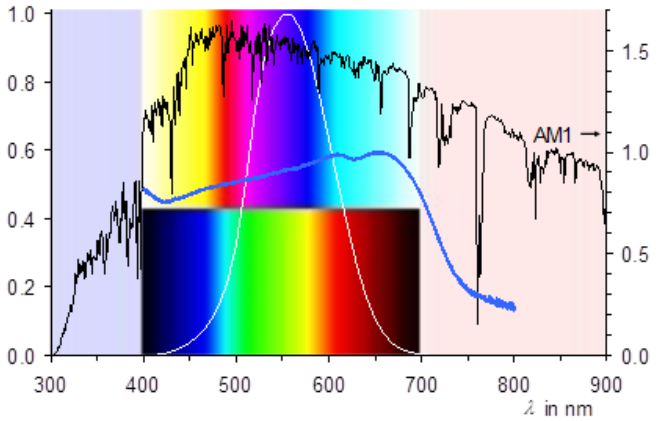


**Figure S1**: *The rainbow spectrum (lower coloured ribbon) and the complementary spectrum obtained for a single absorption band in the visible and white light (upper coloured ribbon), the solar AM1 spectrum (black, noisy curve) and the spectral sensitivity of the human cones for colour vision (white curve). Light blue coloration of denim with indigo as blue curve.*

The impression of colorations with indigo and alizarin can be illustrated of the spectra in **Figure 2**. White solar radiation characterised with the AM1 spectrum (black, noisy curve) forms the rainbow spectrum of the lower coloured ribbon where a dye with a single absorption band removes part of this spectrum and the

complimentary colour of the upper coloured ribbon is obtained. Here one sees deep colours in the middle and the pale colours (yellow and turquoise) at the margins at short and long wavelengths. This is caused by the spectral sensitivity of the human eye where the cones are responsible for colour vision (see white curve in **Figure 2**). As a consequence, the red colour of colorations with alizarin appreciably hit the left shoulder of the bell-shaped sensitivity curve and cause strong colour impressions. Blue colorations are even more effective because they correspond to the right shoulder, not far away from the maximum of sensitivity. However, the spectral shapes of the absorption bands of alizarin and indigo have to be considered for the impression of colour where suitable processes of coloration cause a comparably sharp declining of the absorption spectrum of alizarin at the edge at long wavelengths and cause a brilliant coloration able to compete with modern brilliant red colorations. The absorption spectra or colorations with indigo are much broader as it is shown with the blue curve of a light coloration of denim, and causes a more dull effect. This had to be accepted in Middle Age because of the lack of alternatives and is nowadays wanted for special fashion applications only.

Indigo absorbs at very long wavelengths considering the small chromophore where even the terminal benzo groups are of minor importance because their replacement by an aliphatic structure will cause only a slight hypsochromic shift. The operating of the chromophore can be clearly illustrated by the concept of König and Ismialsky [1, 2]. The centre of **1** is formed by a double bond with crosswise attached amino donor and carbonyl acceptor groups. The combination of donor and acceptor groups themselves would shift the absorption of the double bond to long wavelengths (bathochromic shift). Moreover, the proximity of the donor and acceptor groups cause interrelating electrostatic interactions with amplification of the donor and acceptor aptitudes. Obviously, the resulting donor and acceptor effects in **1** are so far balanced that the absorption at such long wavelengths results; the reported intermolecular hydrogen bonds are less important for the absorption because even homogeneous solutions of **1** and its alkyl derivatives are blue. The balanced donor and acceptor aptitudes may be perturbed by the replacement of the strongly electron donating nitrogen by the weaker donating oxygen with the consequence of a pronounced hypsochromic shift so that oxindigo absorbs light in the UV. The balancing can be re-established by the introduction of amino donor groups into the phenyl groups at the positions 6 and 6' resulting in the expected strong batochromic shift of the absorption into the visible [3, 4]. The action of the bromine atoms in **3** can be interpreted in the same manner because of amplifying the acceptor aptitudes of the carbonyl groups.

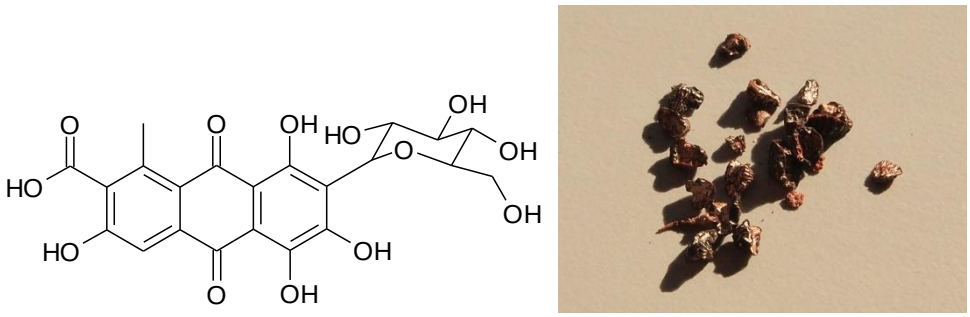


**3**'

**Figure S2:** *Formula of carminic acid (left) and photo of collected cochineal scale insect (Dactylopius coccus C.) for the preparation of 4 (right).*

A purple color was obtained by a hypsochromic shift of the absorption of **1** to form **3**; on the other hand, a batochromic shift of the red **2** might result in a similar color. Possibilities therefore can be illustrated by means of an analysis with König's concept analogously to **3**. There are two carbonyl groups in **2** as acceptors and one

significant OH group in *ortho* position 1 as a donor (the second OH group in the *meta* position 2 is essentially a substituent and of minor importance for the chromophore); thus the chromophore of **2** resembles the basic chromophore of **1** although the chemical structures are completely different where the proximal donor and acceptor group causes an amplification such as in (**1**). The addition of the lacking donor group in position 4 should give an appreciable bathochrommic shift; this is realised in the natural carminic acid (compound (**3'**), RN 1260-17-9) with the two OH groups in the positions 1 and 4; see **Figure S2**. Carminic acid was obtained from insects living around the Baltic See and later-on from cochineal scale insect (*Dactylopius coccus C.*) living on opuntia cactus family in South America because of the appreciable higher content of dye. Carminic acid applied in mordant dying was a substitute for Tyrian purple. Natural carminic acid is still in use for food-near applications.

Thus chlorine was introduced in (**4**) for electron depletion by means of aqua regia at 50°C (this demonstrates also the extraordinarily high stability of the basic structure of (**4**)) to obtain the chloro derivative indanthrene blue GCD (**6**) with improved fastness concerning bleach.

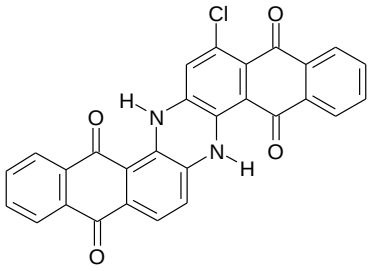


**4'**

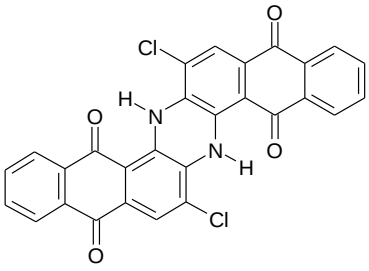


**4"**

The position of the chlorine atom in (**4'**) is not optimal because it is in *ortho* position to a carbonyl group. As a consequence, the *meta* position (position 3) of chlorine was targeted and 2-amino-1,3-dichloroanthraquinone was allowed to react under alkaline conditions with the chloride anion as the leaving group to obtain indanthrene blue BC (**4"**) with further improved properties and wide applications where fastness is an important parameter. The application of König's concept to the chromophore of the mentioned indanthrenes indicate a relationship to (**2**) because of the vicinity of a donor to the carbonyl group as the acceptor where a donor for the second carbonyl group is missing and the much stronger donor aptitudes of an amino group compared with a hydroxy group can cause a further sound bathochromic shift; this can be illustrated both by the fact that the vat of (**4**) is still blue in contrast to indigo that is dark yellow, because the generation of a vat leaves one chromophore untouched (the blue color of the vat generated technical problems in the very beginning of dying with (**4**)) and the introduction of amino groups in postion 4 and 4' causes a further batochromic shift to obtain the green indanthrene green BB; this is in complete analogy to the bathochromic shift from (**2**) to (**4**). Bohn's concept of alkali melt of aromatics for the synthesis of more complex aromatic structure seems to be more general because it was successfully applied to many other systems.

Compound (**5**) exists in several allotropic modifications where colours can be obtained from red to violet also depending on the milling process.

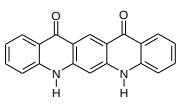


**5'**

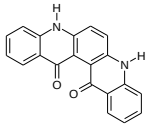


**5"**

Electrostatic interactions between the donor and acceptor groups in (**5**) may be responsible for the deep colour such as in (**1**) whereas contrasting the linear (**5'**) and the angular isomer (**5"**) where no such interactions are possible absorb at appreciably shorter wavelengths and are not applied as dyestuffs. The compounds (**5'**) and (**5"**) exhibit a higher solubility than (**5**), presumably because of less effective hydrogen bonds. The stacking of the chromophores in the crystals of (**5**) additionally cause exciton interactions modulating the colours in the various allotropic modifications to obtain a scale of colours for the pigments. The substitution of aniline as the precursors of (**5**) allows the efficient introduction of various groups into (**5**). The latter forms a tautomer with a donor-acceptor substituted carbonyl enamine where the *ortho* positions of the electron rich phenyl rings react with the electrophilic carbonyl groups of the esters under the rough reaction conditions. Thus, a broad spectrum of compounds is available for the modern application of chromophores.

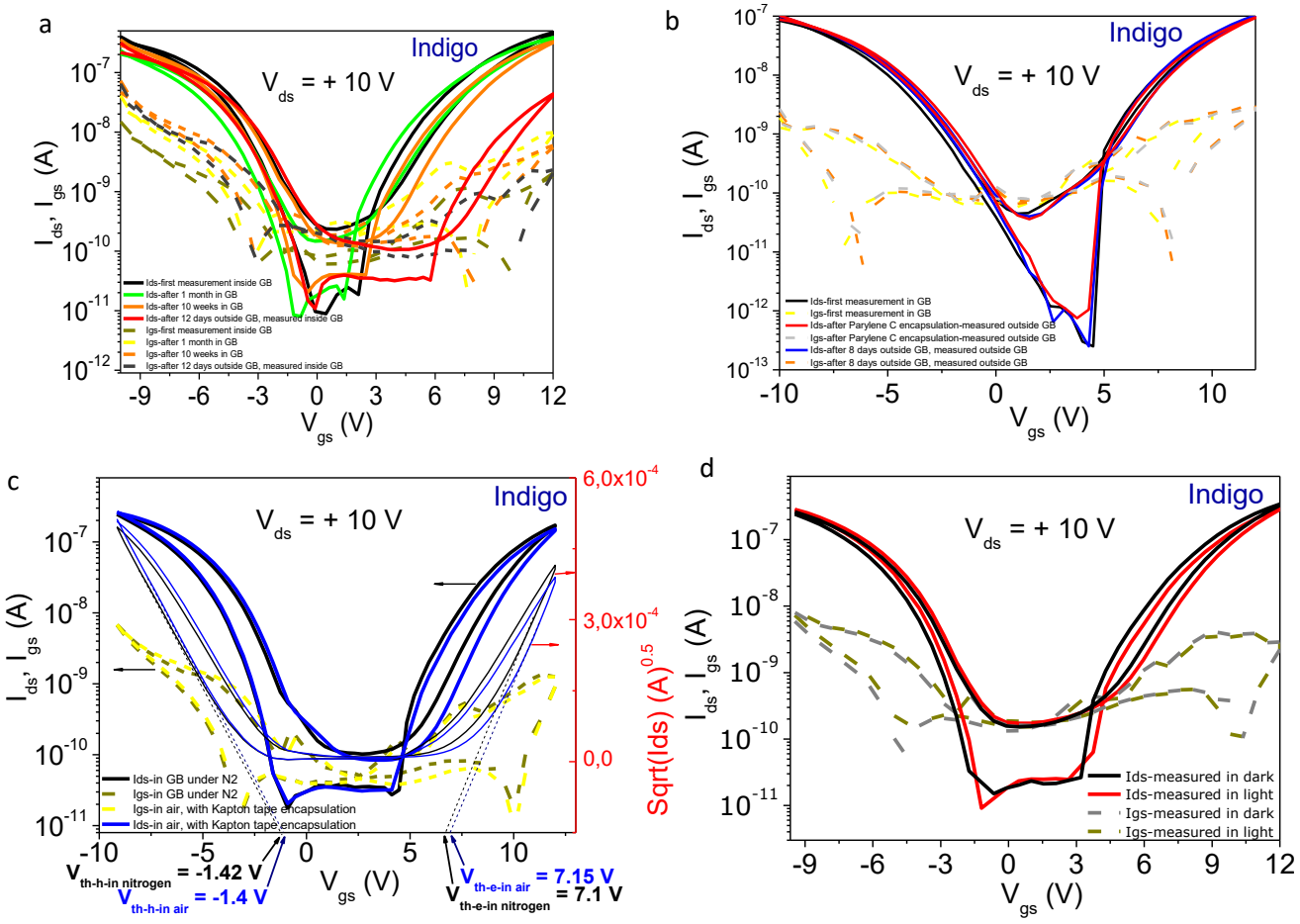


**Figure S3**: *Transfer characteristics of OFETs with Indigo semiconductor on Al gate, AlOx-Tetratetracontane dielectric, and Au source and drain electrodes.* ***a)*** *Investigation of stability to air exposure for Indigo-based OFETs: first measurement in glove box for a sample never exposed to air (black line), measurement in glove box after 30 days of storage in glove box (green line), measurement in glove box after 70 days of storage in glove box (orange line) and measurement in glove box after exposing the sample for 12 days to ambient air (red line). This sample was never measured outside glove box;* ***b)*** *Stability to measurement in air after encapsulation of the device with vacuum deposited parylene C: first measurement in glove box as reference (black line), measurement outside glove box after parylene C encapsulation (red line) and measurement outside glove box after 8 days exposure of the device to ambient air (blue line);* ***c)*** *measurement inside glove box (black line) and outside glove box (blue line), after straight forward encapsulation of the device with poly imide tape (commercial Kapton tape);* ***d)*** *Stability to illumination of a device measured in glove box under complete darkness (inside a closed measurement box) and under illumination by a combined glove box light (top) and a simulated AM1.5 solar irradiation using a Steuernagel 575 sun simulator with 100 mW/cm² intensity.*

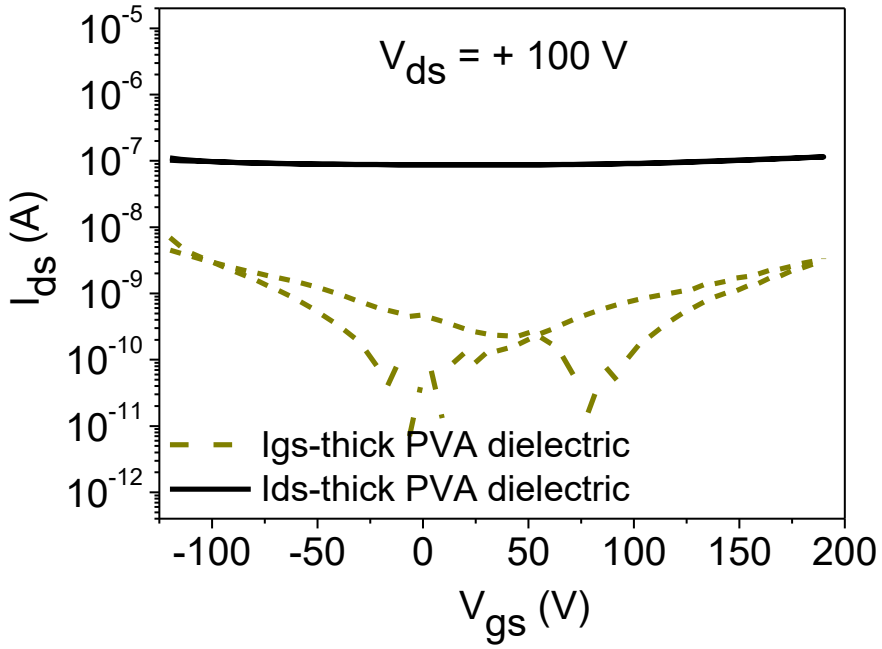


**Figure S4**: *Thick PVA dielectric for Tyrian purple OFET. NO OFET characteristic is obtained on PVA, a polar dielectric.*

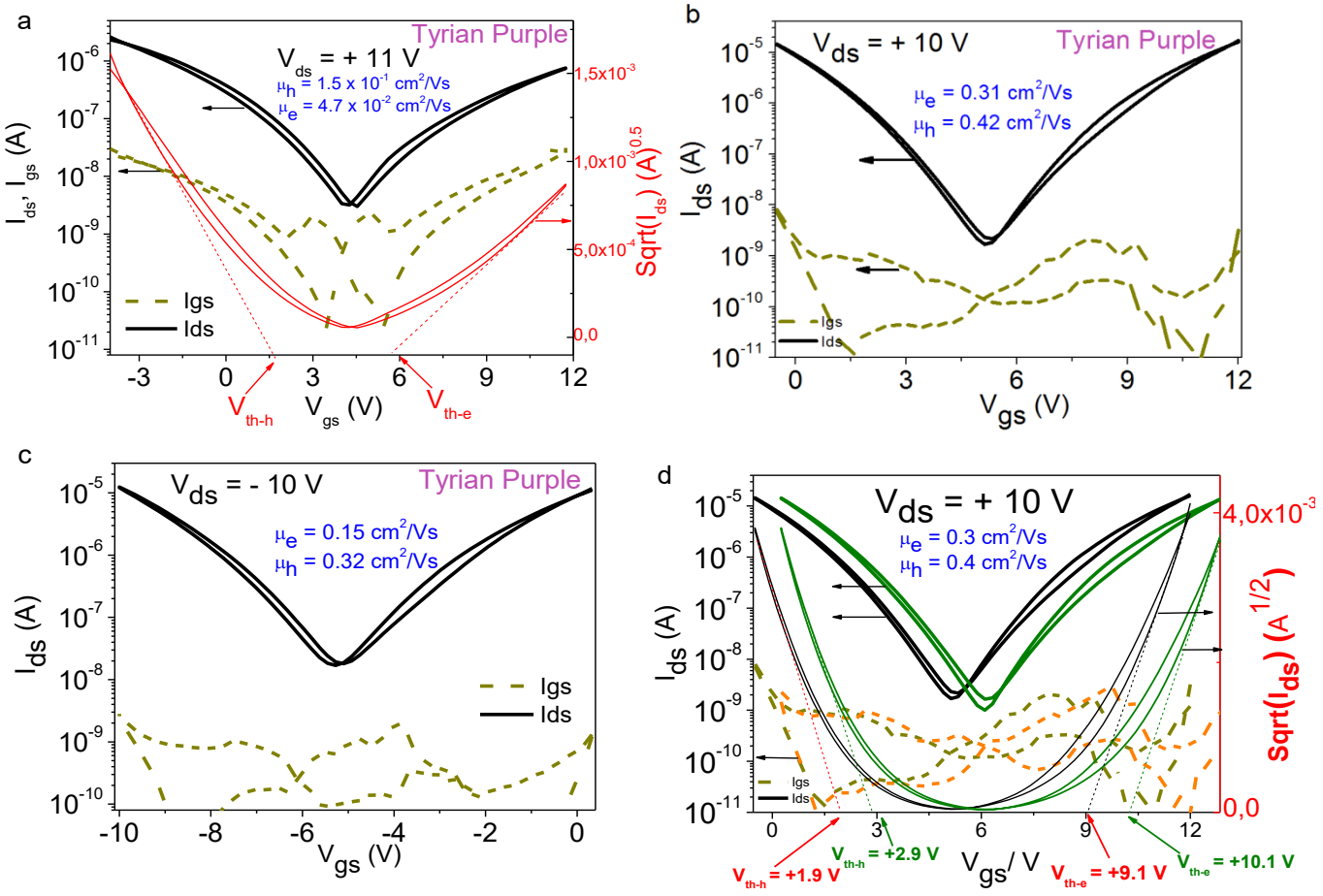


**Figure S5**: **a)** Transfer characteristic obtained after slow deposition of top gold contacts (deposition rate between 0.05 to 0.1 nm/sec), showing the characteristic lower performance of the electron channel; ***b)*** *and c) Transfer characteristics of the same OFET measured at negative Vds (panel c)) and positive Vds (panel d), in the case of fast deposition of the top gold contact electrodes (deposition rate greater than 1 nm/sec, but lower than 1.5 nm/sec). Transfer characteristics of OFETs with Tyrian purple (6,6'-Br-Indigo) semiconductor on Al gate, AlOx-Tetratetracontane dielectric, and Au source and drain electrodes.* ***d)*** *A sample initially measurement in glove box (black line) and measured in glove box after the sample was exposed (but not measured) to ambient air, showing excellent stability to operation in terms of mobility, but not threshold voltage immovability.*

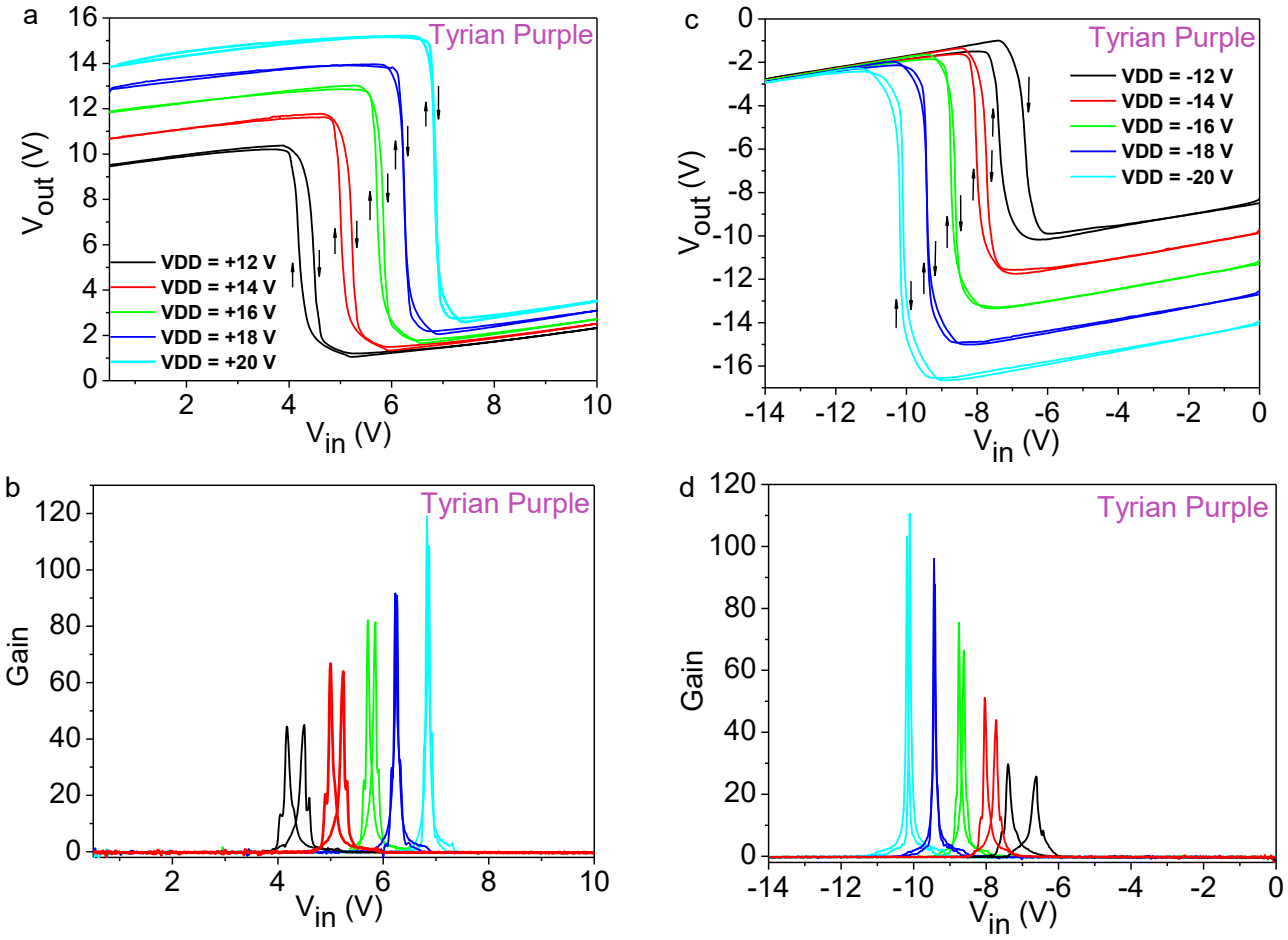


**Figure S6:** *Complementary-like inverters with Tyrian purple semiconductor obtained by connecting two OFETs featuring a common gate electrode.* ***a)*** *Inverter transfer characteristic at various $V_{dd}$ voltages in the positive quadrant, measured at a frequency of 1 MHz;* ***b)*** *the respective inverter gains of the characteristics displayed in a), in the positive quadrant;* ***c)*** *Inverter transfer characteristic at various $V_{dd}$ voltages in the negative quadrant, measured at a frequency of 1 MHz;* ***d)*** *the respective inverter gains of the characteristics displayed in c), in the negative quadrant.*

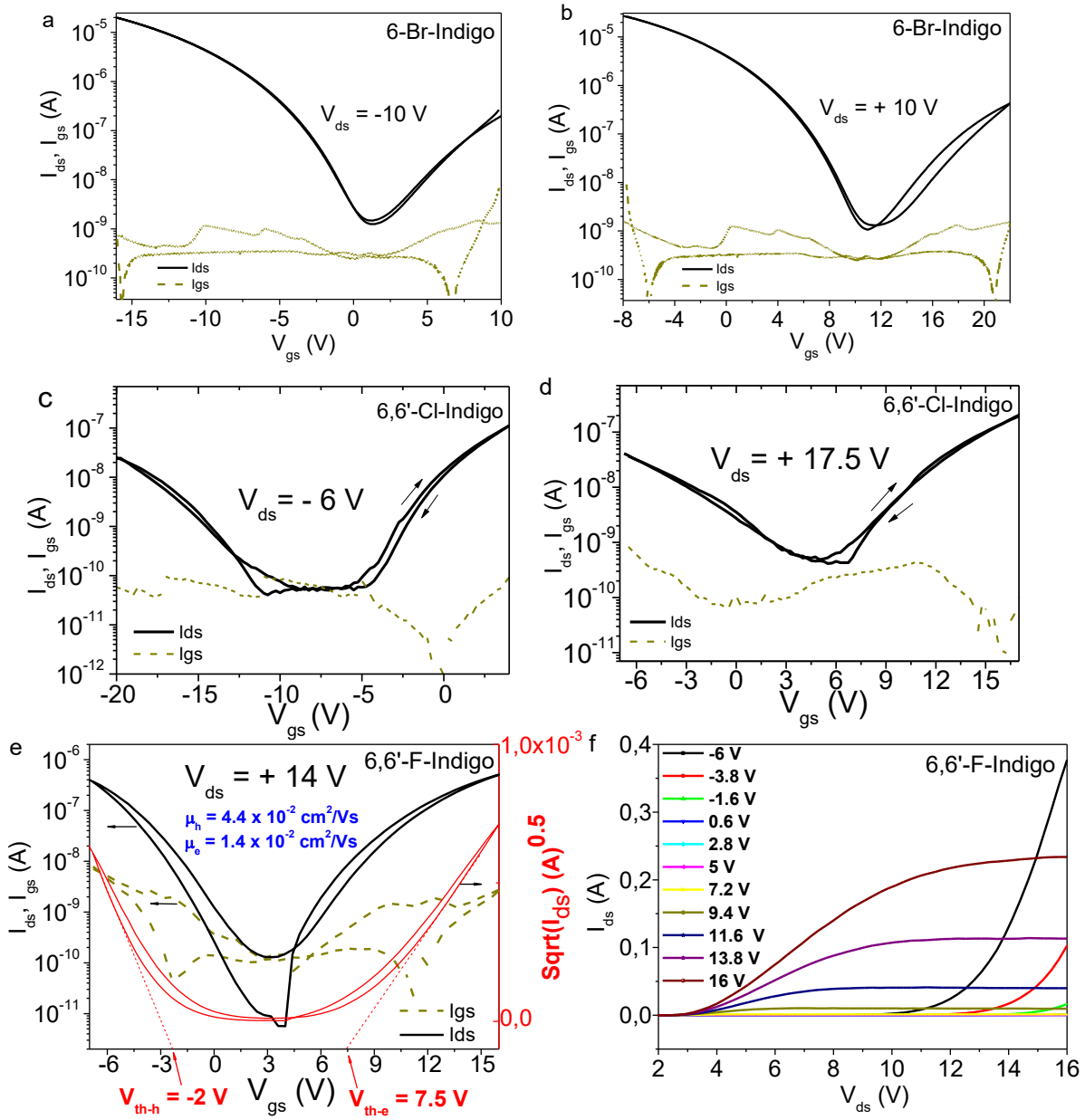


**Figure S7:** *Transfer and output characteristics of OFETs with three different indigo derivatives as semiconductors on Al gate, AlOx-Tetratetracontane dielectric, and Au source and drain electrodes, showing a large variation in performance and their generated characteristics. All devices are fabricated on a structure comprising Al gate, AlOx-Tetratetracontane dielectric, and Au source and drain electrodes.* ***a)*** *Transfer characteristics of monobromo-Indigo measured with positive drain voltage and* ***b)*** *Transfer characteristics of monobromo-Indigo measured with negative drain voltage. In both cases, a lower performance of the electron channel is recorded;* ***c)*** *Transfer characteristics of 6,6'-Cl-Indigo measured with negative drain voltage and* ***d)*** *Transfer characteristics of 6,6'-Cl-Indigo measured with positive drain voltage. In both cases a lower performance of the hole channel is observed. Reproduced with permission from Ref. [83]: Petritz, A.; Fian, A.; Głowacki, E. D.; Sariciftci, N. S.; Stadlober, B.; Irimia-Vladu M. Ambipolar Inverters with Natural Origin Organic Materials as Gate Dielectric and Semiconducting Layer. Phys. Status Solidi (RRL) 2015, 9(6), 358-361. Creative Commons Attribution license: https://creativecommons.org/licenses/by/4.0/. Copyright 2015, Wiley-VCH;* ***e)*** *Transfer characteristics of 6,6'-F-Indigo measured with positive drain voltage showing a very good balance of the electron and hole channels in terms of mobility and hysteresis; and* ***f)*** *Output characteristics of 6,6'-F-Indigo measured in the positive quadrant showing super-linear increase of the drain current at low gate voltages, a typical print of ambipolar semiconductors. The devices with Br-Indigo and 2F-Indigo had AlOx+TTC dielectric. The devices with 2Cl-Indigo had AlOx+trimethyl silyl cellulose (TMSC) dielectric.*

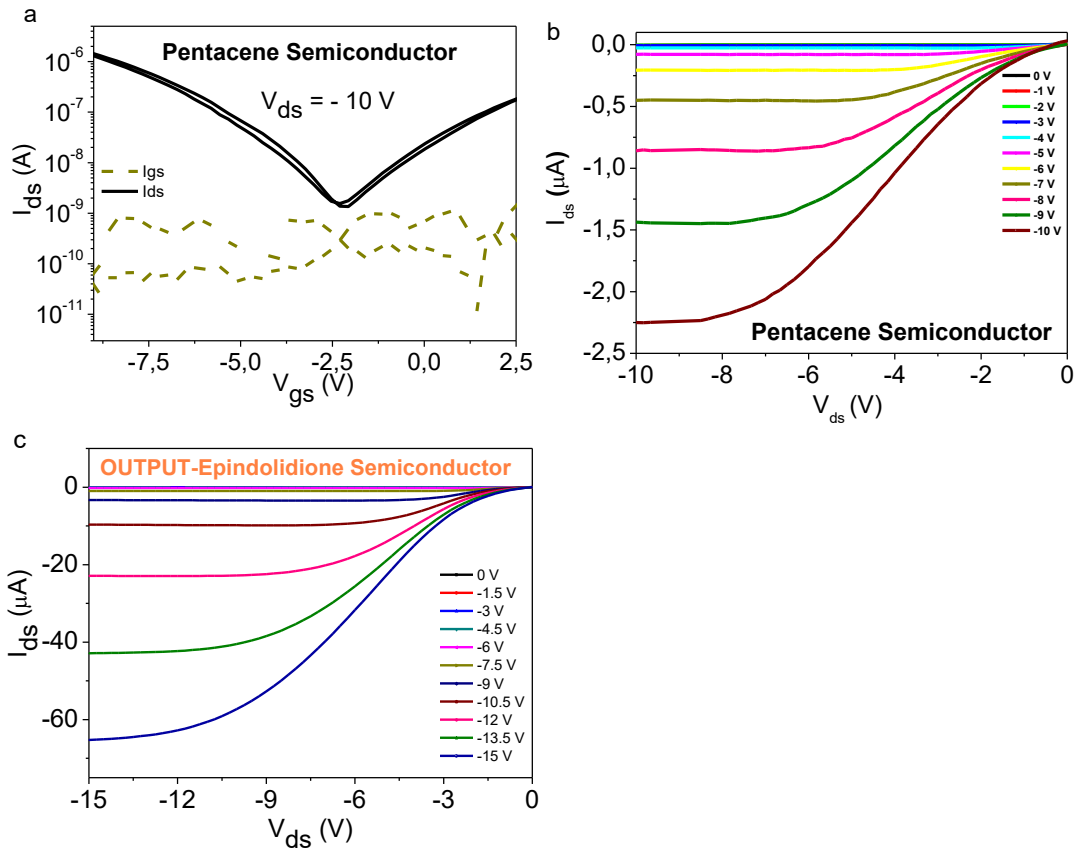


**Figure S8: a)** Transfer characteristic of a Pentacene channel OFET where gold was evaporated at a constant rate of 0.01 nm/sec. The sample shows ambipolar charge transport; **b)** Output characteristic of the OFET sample with Epindolidione channel presented in **Figure 5 a)**

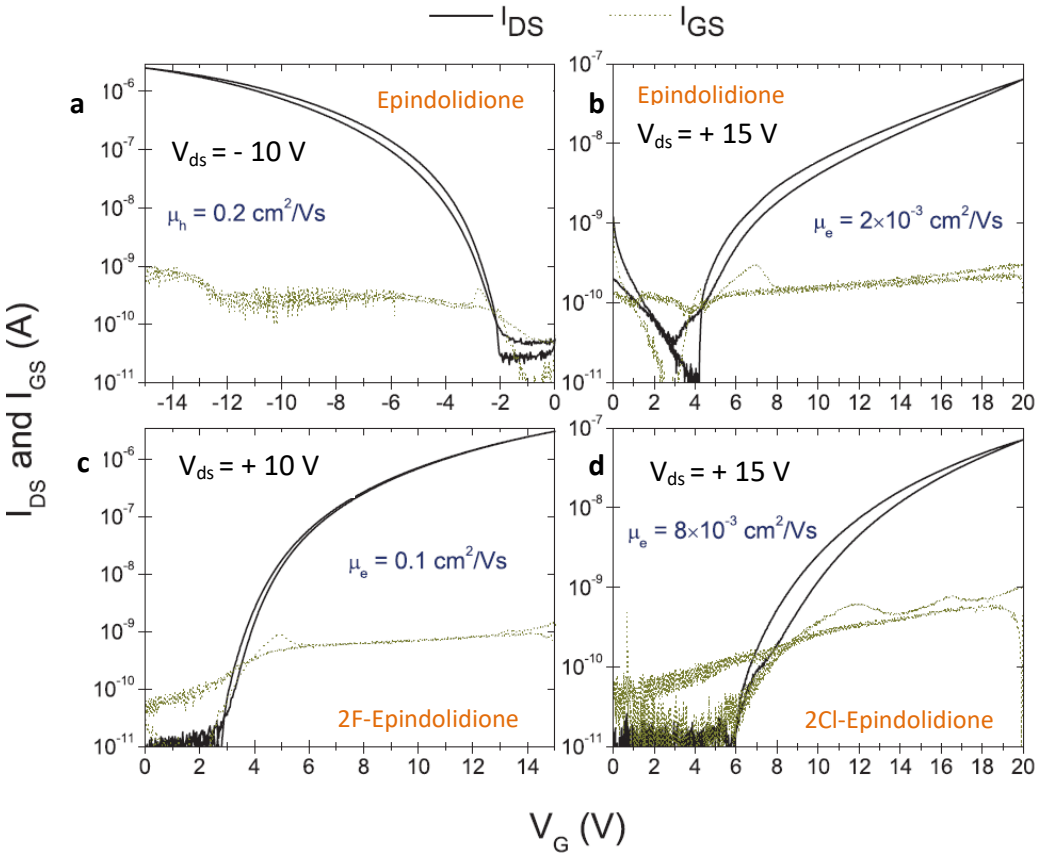


**Figure S9:** *OFET transfer characteristics for **a)** Epindolidione OFET on Al gate, AlOx-Tetratetracontane dielectric, and Au source and drain electrodes showing the typical occurrence of the hole channel; **b)** A similar Epindolidione OFET geometry as in panel a) but with Al source-drain electrodes showing the rise of electron channel **c)** 2F-Epindolidione semiconductor for an electron (n-type) operating OFET with Al source and drain electrodes; and **d)** 2Cl-Epindolidione semiconductor for an electron (n-type) operating OFET with Al source and drain electrodes.*

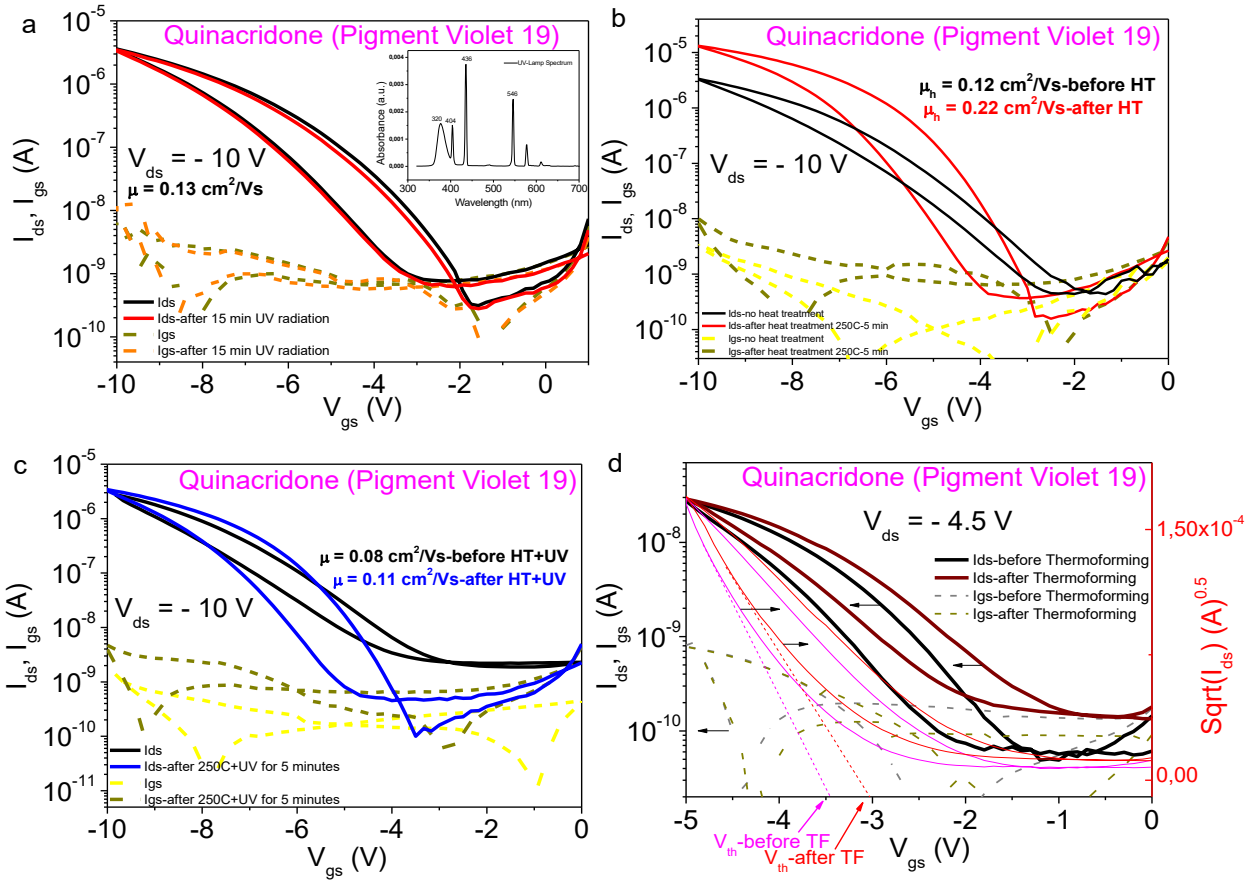


**Figure S10:** *Transfer characteristics of OFETs with Quinacridone (Pigment Violet 19) semiconductor on Al gate, AlOx-polyethylene dielectric, and Au source and drain electrodes. The samples in panels a)-c) were fabricated on glass substrates and the polyethylene was crosslinked by a combination of 30 minutes UV radiation and heating at 110 ℃ prior to the quinacridone vacuum deposition; the sample in panel d) was fabricated on polycarbonate foil and the polyethylene was not crosslinked.* ***a)*** *Stability of OFET characteristics after 15 minutes exposure to UV-radiation inside glove box. Both transfer curves were measured inside glove box. The inset displays the UV spectrum of the lamp employed in the test;* ***b)*** *Transfer characteristics of an OFET before and after 5 minutes exposure to 250 C on top of a hot plate inside the glove box, showing a significant increase in mobility after the heat treatment, albeit with an increase in hysteresis;* ***c)*** *Combination of the two tests (UV radiation and temperature) for another OFET. The test was conducted inside glove box;* ***d)*** *Transfer characteristics of a quinacridone OFET before and after Thermoforming process. The sample in panel d) withstood a temperature of 110 ℃ and a pressure of 100 bar for a time of 3 seconds during the thermoforming process. The sample shows a minimal decrease in semiconductor mobility after thermoforming, accompanied by a 0.5 V threshold voltage shift.*

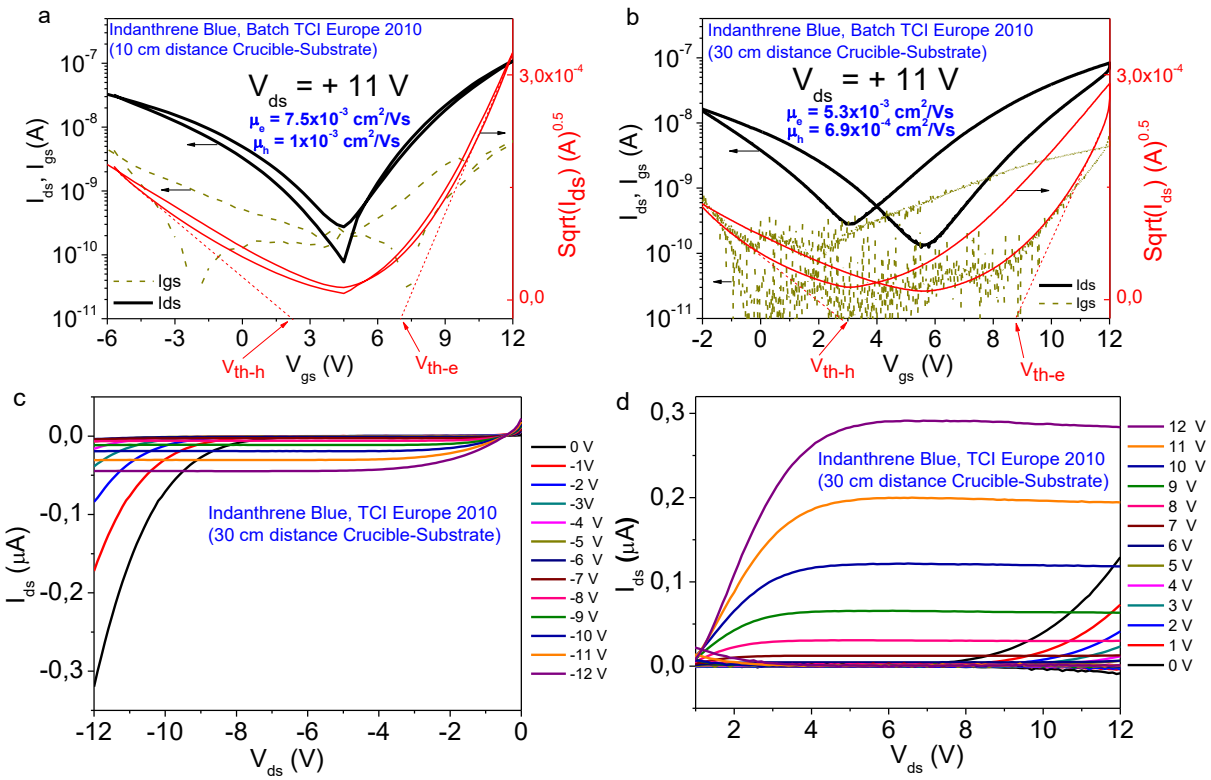


**Figure S11:** *Transistor characteristics (transfer and output) of OFETs with Indanthrene Blue (Vat Blue 4) semiconductor on Al gate, AlOx-tetratetracontane dielectric, and Au source and drain electrodes.* ***a)*** *Transfer characteristics obtained for an OFET with Indanthrene Blue deposited from a crucible with 10 cm distance from substrate holder;* ***b)*** *Identical transistor geometry and deposition conditions with the device in panel a), but with the distance of 30 cm between crucible and substrate holder;* ***c)*** *and* ***d)*** *Output characteristics in the negative (c) and positive (d) quadrant of the device displayed in panel b). OFET showed in panel a) was produced in the year 2011, while OFET showed in panels b-c-d) in the year 2018 from the same precursor powder, purified 3 times and stored in glove box under Argon all the time. The same masks, dielectric layers and transistor geometry were employed in the two OFETs fabrication.*

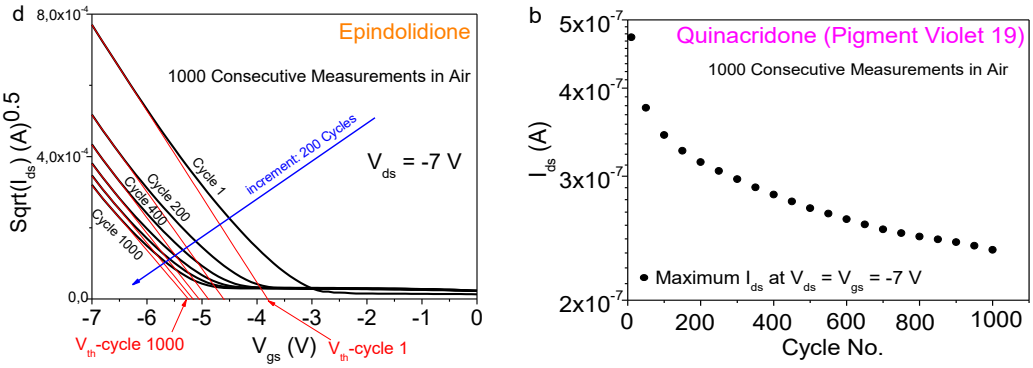


***Figure S12:*** *Epindolidione and Quinacridone OFETs subjected to 1000 consecutive cycles in air.* ***a)*** *Epindolidione OFET showing a significant threshold voltage shift during the test, with every 200$^{th}$ cycle being displayed;* ***b)*** *Quinacridone OFET showing a factor of 2 decline in absolute drain current during the test, with the Ids value of every 50$^{th}$ cycle being displayed.*

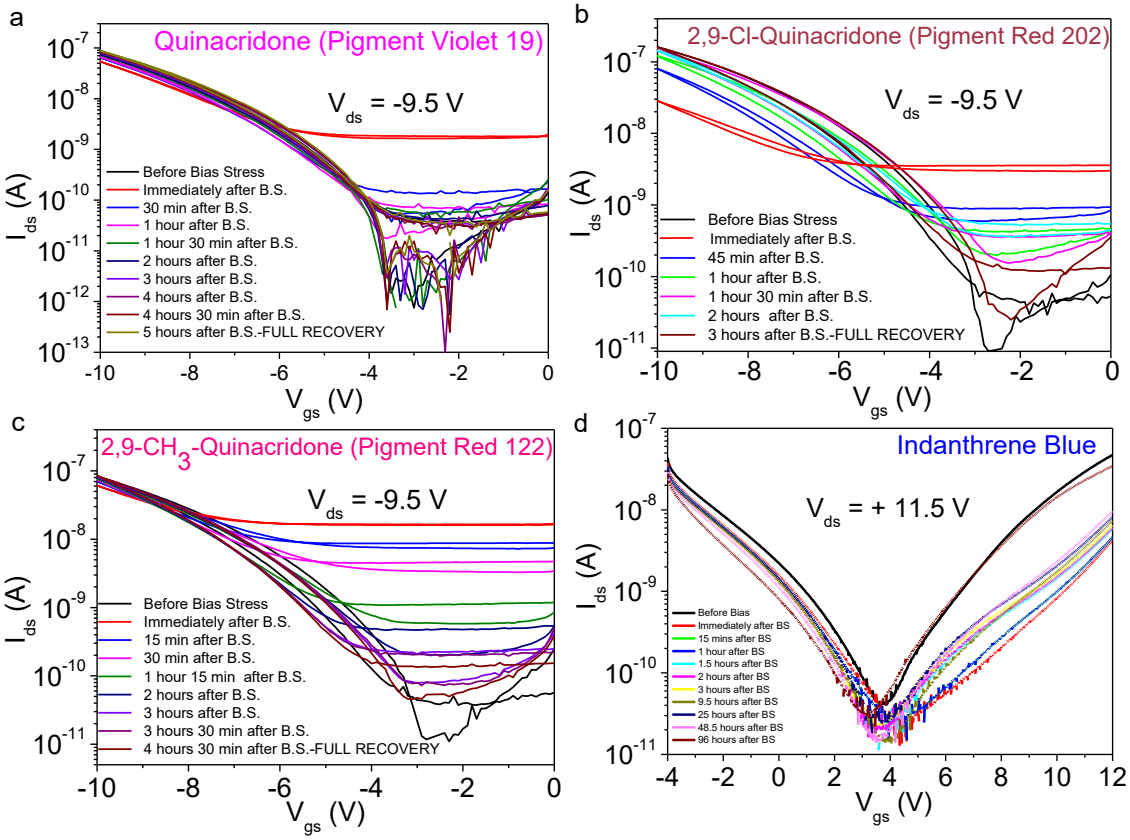


**Figure S13:** *The behavior of the transfer characteristics before and after bias of 14.5 hours:* ***a)*** *Quinacridone OFET;* ***b)*** *dichloro-Quinacridone OFET;* ***c)*** *dimethyl-Quinacridone OFET;* ***d)*** *The behavior of the transfer characteristics before and after bias of 14.25 hours of Indanthrene Blue OFET, batch of TCI Europe. All samples were fabricated on Al gate, AlOx-pentacontane dielectric, and Au source and drain electrodes. In panel d) only unidirectional curves are shown, in order to avoid cluttering the graph.*

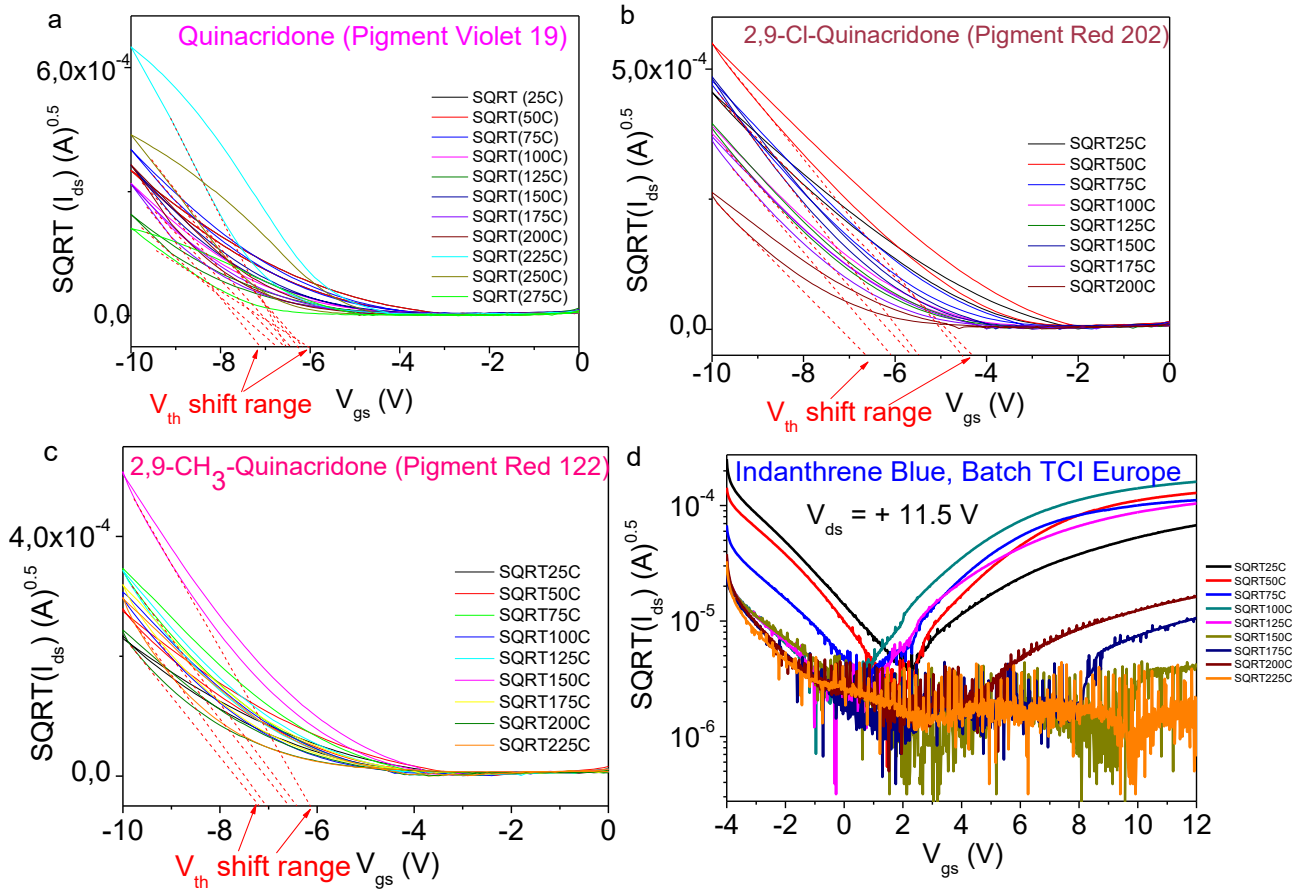


**Figure S14**: *Square root value of the $I_{ds}$ currents of the annealed OFET devices displayed in* ***Figure 11***.

[1] König W. Über den Begriff der „Polymethinfarbstoffe" und eine davon ableitbare allgemeine Farbstoff-Formel als Grundlage einer neuen Systematik der Farbenchemie. *J. Prakt. Chem.* **1925**, *112*, 1–36.

[2] Ismailsky, W. Ph.D. Thesis, University of Dresden, **1913**.

[3] Langhals, H.; Wagner, B. Oxindigo: Farbvertiefung, starke Fluoreszenz und großer Stokes-Shift durch Donorsubstitution. *Angew. Chem.* **1996**, *108*, 1090-1093.

[4] Langhals, H. Wagner, B. Oxindigo: Colour Deepening, Strong Fluorescence and Large Stokes-Shift by Donor-Substitution. *Angew. Chem. Int. Ed. Engl.* **1996**, *35*, 1016-1019.